RELATIVE PERMEABILITIES FOR THE PRODUCTION OF SOLUTION GAS FROM WATERFLOOD RESIDUAL OIL

C.A. Grattoni, R.I. Hawes and R.A. Dawe*

Centre for Petroleum Studies, T.H. Huxley School, Imperial College, London SW7 2AZ, UK
* College of Engineering, University of Qatar, Doha, Qatar, Arabian Gulf

ABSTRACT

Earlier experiments have shown that when solution gas is released from waterflooded residual oil by depressurisation, the gas becomes mobilised when the critical gas saturation has been reached, but the gas saturation continues to increase as more gas is generated. The saturation of the gas remaining in the pore space at the end of the depressurisation is an important parameter in determining the economic performance of any depressurisation application since it represents an amount of gas that cannot be recovered. Its magnitude depends upon the rate of gas generation and the gas relative permeabilities.

Experiments have been performed to measure water and gas relative permeabilities when gas is released from solution by heating a solution of pentane dissolved in a non volatile heavy paraffin. The measured relative permeabilities were extremely low in both cases; the water relative permeabilities being of order 10^{-2}, whilst the corresponding values for the gas phase were in the range 10^{-5} to $10^{-3,}$ which is an order of magnitude lower than would be predicted using a Corey type equation for the non-wetting phase. The results suggest that gas relative permeabilities measured in gas-water displacement experiments are not applicable to the depressurisation of waterflooded reservoirs.

Visual observations of the flow behaviour in glass micromodels have shown that the low values of gas relative permeabilities can be explained by the fact that the filaments which form the channels for gas flow are not stable, and that the flow is intermittent. As a result, the effective total area for flow at any particular gas saturation is substantially reduced, thus reducing the permeability to the gas.

The results of the experiments suggest that network models that have been developed for predicting oil-water and gas-water displacement relative permeabilities are not directly applicable to situations in which gas is released from solution by depressurisation. To provide a suitable model for calculating relative permeabilities in these situations, new algorithms need to be introduced into the network models to represent the cyclical nature of filament rupture and reformation.

INTRODUCTION

Much of the published research concerning the depressurisation of reservoirs after they have been waterflooded has focused upon the evaluation of the critical gas saturation at which gas released from solution first becomes mobilised (1-9). Results from high pressure experiments using reservoir oils, as well as simple mixtures of alkanes, have been reported by researchers at the Shell laboratories at Rijswijk (1-4), and these results have been used to assess the

performance of the process in the Brent reservoir (4). In our own laboratory, the physical mechanisms of nucleation, growth, and mobilisation of gas released from solution have been studied (5-7), and a mathematical model to describe the behaviour and predict critical gas saturation was developed (8), which was shown to be consistent with the results from the high pressure experiments. More recently (9), McDougall and Sorbie have published a paper describing a network model that uses a similar approach to that described in (8), and have devised a scaling group to correlate the effect of the operating parameters on the critical gas saturation.

Our attention has now turned to the behaviour that occurs during the continuing period of depressurisation after the critical gas saturation has been reached. Some of our earlier experiments showed that although gas started to flow out of the test section when the gas saturation reached the critical value of 9%, the gas saturation continued to increase as more gas came out of solution, ultimately reaching a value of 30% (7). Scherpenisse et al (3) observed a similar effect in their high pressure experiments using reservoir oils and rock materials. In an experiment with a depressurisation rate of 4 bar/hr, the gas was first mobilised when its saturation reached the critical value of about 22%, but the gas saturation in the core continued to rise during the later stages of the depressurisation, reaching 32% at the end of the experiment. At the same time, the total hydrocarbon (gas + oil) saturation increased from 44% to 53%.

Ligthelm et al (4) used the term “ultimate” gas saturation for the amount of gas that remained in the pore space of the rock at the end of the depressurisation. It is an important parameter in determining the economic performance of any depressurisation application, since this amount of gas cannot be recovered from the reservoir. Its magnitude will depend upon the rate of gas generation (i.e. the rate of pressure reduction) and the gas relative permeability once the gas has become mobile. At present there is virtually no published experimental data concerning gas relative permeabilities in these circumstances. Ligthelm et al used a Corey type relationship for the gas/hydrocarbon relative permeabilities when simulating the reservoir conditions depressurisation experiments. However, it should be noted that in the only comparison between simulation predictions and experimental results presented in their paper, the simulation model under predicts the ultimate gas saturation obtained in the experiment by about 10 percentage points, which suggests that the actual gas relative permeability in the experiment was much lower than that used in the simulation.

McDougall and Sorbie used their network model to investigate possible theoretical relationships between gas relative permeability and gas saturation (9), and suggested that the scaling group that they derived for estimating the critical gas saturation could be used to re-normalise gas flood relative permeability curves for use in depressurisation field simulations. If this were proved to be correct, it should be possible to derive a suite of relative permeability curves, covering a range of depressurisation rates, from a single external drive laboratory experiment.

In view of the paucity of information concerning gas relative permeabilities during solution gas release, an experimental study is being undertaken in this laboratory. The following paper presents the results from the first part of this study.

EXPERIMENTAL APPROACH

The experiments were performed using a cylindrical beadpack of 2.5 cm diameter and 22 cm length, containing more than 300,000 randomly packed beads 0.65 to 0.75 mm in diameter with an absolute permeability of 6 Darcies and a pore volume of 38.4 cm^3. These packs provide a simplistic representation of the main flow characteristics of porous rocks, and had the additional merit of being transparent, so that any movement of the fluids could be observed. The glass surfaces of the models were strongly water-wet. A diagram of the experimental arrangement is shown in Fig. 1. The outlet of the test section was connected to a separator, which consisted of two calibrated and concentric glass tubes, where the production rate of each fluid phase could be measured. The produced oil and water were collected and measured in the inner tube whilst the gas was collected and measured in the outer tube. The whole of the apparatus was mounted vertically in a temperature controlled bath, as shown. All the measurements were taken at atmospheric pressure. As the maximum pressure difference was of 1 kPa, the test section was also effectively at atmospheric pressure.

As in our previous experiments, the oleic phase was a simple hydrocarbon mixture consisting of n-pentane dissolved in heavy paraffin (non-volatile). Whilst gas is released from solution by reducing the pressure below the bubble point in a reservoir application, the simpler procedure of heating the mixture to liberate gas from the oil phase was adopted for the experiments, see Fig. 2. The three phase mixture that was created had a positive spreading coefficient.

At the start of an experiment, the beadpack was first filled with CO_2 and flooded with degassed water until it was fully saturated. It was then flooded with oil to connate water saturation and re-flooded with water to produce a residual oil saturation. The temperature of the water bath was then slowly increased at constant rate, starting at around 30 ^oC to release the pentane gas from solution, and the accumulated volumes of each of the effluent fluids were measured. These volumes were corrected at each temperature to allow for the combined thermal expansions within the pack and the change in pore volume. The corrected data were then used to determine the average saturation of the phases and the flow rates.

The differential water pressure across the pack was continuously measured and recorded using a gas filled pressure transducer that was connected to water filled lines that were attached to the top and bottom of the test section, as shown. At each stage of the experiment, the water levels in these lines were adjusted to a pre-determined reference position, thus compensating for the hydrostatic head within the bead pack.

EXPERIMENTAL RESULTS

The accumulated volumes of the individual components produced from the beadpack for heating rate of 2 ^oC per hour are shown in Fig. 3 A and B as a function of the gas saturation, Sg. An approximate rate of pressure reduction can be estimated from the gas evolution shown in Figure 3 B. The rate of gas production is comparable to that which would be produced if oil from one of the North Sea reservoirs were to be depressurised at a normalised rate of pressure reduction of 10^{-2} to 10^{-1} $(P_B\text{-}P)/(P_B.\text{hr})$ where P_B is the bubble point pressure. Whilst these rates of depressurisation may be three orders of magnitude greater than field rates, they are of the same order as the depressurisation experiments reported by Braithwaite et al (2).

In the initial stages, only water was collected in the separator, and no gas or oil was produced until the gas saturation reached a critical value of about 10%, at which stage gas and a small amount of oil started to flow out of the test section. This is consistent with the behaviour observed in our earlier studies. Note that although gas was mobilised when its saturation reached 10%, the saturation continued to increase as more gas was released from solution, ultimately reaching a value of 23%.

The rates at which water and gas flowed out of the test section are presented as a function of the gas saturation in Fig. 4a, and the differential pressure measured for the water phase is plotted in Fig. 4b. It can be seen that the water flow rate increased during the early stages of the experiment, when the gas remained immobile, but once the critical gas saturation had been attained, the amount of water displaced decreased as the flow of gas increased. By the time that the gas saturation had reached 23%, the flow of water out of the test section was negligible. The measured differential pressure in the water phase followed a similar pattern, although the decrease in pressure drop after the critical gas saturation was slower than the decrease in water flow rate, because of the additional resistance to flow created by the increasing gas saturation.

ANALYSIS OF RESULTS

The results were used to generate relative permeability curves for both the gas and water phases as a function of gas saturation. In performing this analysis, it was recognised that gas was being released from solution over the whole length of the test section, so that for both phases the flow rate increased with distance from the bottom of the beadpack. For the water phase, the flow equation for any position h from the bottom is given by:

$$\left(\frac{dP_w}{dh}\right)_h = r_w.\, g + \frac{m_w}{K.\, k_{rw}.\, A}\int_0^h q.dh \qquad [1]$$

where P_w is the pressure in the water phase, h is the distance from the bottom of the pack, r_w is the water density, $\boldsymbol{g}$ is the gravitational constant, m_w is the water viscosity, K is the permeability of the beadpack, k_{rw} is the water phase relative permeability, A is the cross sectional area, q is the volumetric rate of gas generation per unit length at any location.

If it is assumed that the rate of gas generation per unit length is constant, Equation 1 can be solved for the whole length of the beadpack, and re-arranged to provide an expression for the water relative permeability:

$$k_{rw} = \frac{Q_w m_w.}{2.K.A}.\frac{h_{pack}}{(P_{wb} - P_{wt}) - r_w.g.h_{pack}} \qquad [2]$$

where Q_w is the water flow rate out of the beadpack, and the subscripts b and t refer to the bottom and top of the pack respectively.

As discussed above, the method of measuring the water phase differential pressure already takes into account the hydrostatic head within the pack, so that the measured differential pressure is equal to the group $[(P_{wb} - P_{wt}) - r_w.g.h_{pack}]$. Since this is the pressure differential

that promotes the water flow within the pack, it is referred to as ΔP_{wf}. Hence:

$$k_{rw} = \frac{Q_w.m_w}{2.K.A}.\frac{h_{pack}}{\Delta P_{wf}} \quad [3]$$

A similar equation can be written for the gas phase relative permeability. However, in this case the differential pressure is:

$$\Delta P_{gf} = \Delta P_{wf} + \Delta r.g.h_{pack} + \Delta Pc_{og} + \Delta Pc_{ow} \quad [4]$$

where Δr is the water gas density difference, and ΔPc_{og} and ΔPc_{ow} are the differences between the oil-gas, and oil-water, capillary pressure at the bottom and top of the beadpack respectively. When performing the analysis, the assumption has been made that these differences in capillary pressure are negligible.

The calculated water and gas relative permeabilities are presented in Fig. 5. It can be seen that in both cases the values are extremely low, the water relative permeabilities being of order 10^{-2}, whilst the corresponding values for the gas phase were of order 10^{-5}-10^{-4}. For this reason the measured flow rates and differential pressures were checked and re-checked to ensure that they are correct.

In Fig. 6 the calculated gas relative permeabilities are compared with predictions using a Corey type equation for the non-wetting phase that has been re-normalised to allow for the residual oil saturation, and for the fact that the gas phase relative permeability is zero when the gas saturation is less than the critical gas saturation:

$$k_{rg} = k_{rh,cw}.\left(S_g - S_{gc}\right)^3.\frac{\left[2.\left(1 - S_{wc} - \left(S_o + S_g\right)_{crit}\right) - \left(S_g - S_{gc}\right)\right]}{\left(1 - S_{wc} - \left(S_o + S_g\right)_{crit}\right)^4} \quad [6]$$

Where $k_{rh,\,cw}$ is the hydrocarbon relative permeability at connate water which was measured to be 0.83. Starting with a zero relative permeability at 10% gas saturation, the experimental data and the Corey equation rapidly diverge as the gas saturation increases, and for much of the range of gas saturation the experimental values are an order of magnitude lower than the Corey predictions.

Similar low values of gas and water relative permeabilities were measured by Fishlock et al. (10) in depressurisation experiments performed using cores containing gas at the waterflood residual condition. As a preliminary to their experiments, primary drainage gas-water relative permeability curves were measured in a dynamic displacement experiment, and the results were combined with steady state measurements to provide reference data for the depressurisation experiments. Imbibition curves were calculated using the Land model. When the pressure was reduced, the gas saturation increased from its residual value of 35% to a critical value of 49% before the gas became mobile. Even when the saturation exceeded this threshold value, however, the gas relative permeability did not increase very rapidly, and at a gas saturation of 59%, the measured gas relative permeability was only 0.001, which was more than two orders of magnitude lower than the value of 0.55 measured for the primary drainage gas relative permeability at this gas saturation. The corresponding water relative

permeabilities were in the range 0.03 to 0.01 whilst the gas remained immobile, reducing to about 0.004 at a gas saturation of 59%.

VISUAL OBSERVATIONS

In order to explain the very low values of gas relative permeabilities obtained in the current experiments, some earlier video recordings of the release of solution gas from waterflood residual oil in glass micromodels have been re-examined. The original objective of these early experiments was to study the mechanisms involved during the period when the gas remained immobile, and the development of the critical gas saturation, but the experiments had been allowed to continue after gas had become mobile, and the flow behaviour during this period had also been recorded.

The early studies showed that the gas was mobilised when adjacent bubbles became connected to form continuous filaments or channels through which the gas could flow. Fig. 7-A shows a picture of one of these continuous gas filaments which was taken from the video recording. When the flow characteristics after the gas had been mobilised were examined, it was observed that the filaments were not stable, and that the flow of gas through the channels was intermittent, as is illustrated by the sequence of pictures presented in Fig. 7. Fig. 7-B shows that at some stage the continuous filament was ruptured, and when this happened the pores became invaded by water, Fig. 7-C, so that the flow of gas through this region was interrupted. Some time later, after more gas had been released from solution, gas started to percolate back into the region, Fig. 7-D, and eventually the filament was restored, Fig. 7-E, so that gas could flow through the channel once more. This cycle of filament rupture and reforming was seen to occur quite frequently throughout the remainder of the experiment, and it was also observed to occur in all parts of the porous matrix. The behaviour is due to the interplay between interfacial forces and gravity. Since the pore sizes of the micromodel were of the same order as those in reservoir rocks, similar behaviour can be expected within the reservoir.

Because of the frequent rupturing of the gas filaments within the matrix, only a fraction of the channels that had been formed were actually being used for gas flow at any particular time. As a result, the effective permeability to the gas was substantially reduced, and this was reflected in the measurements taken in the beadpack experiments.

CONCLUSIONS

The experiments have produced very low values of gas relative permeabilities for the case of solution gas being released from waterflood residual oil, which are up to an order of magnitude lower than were calculated using correlations based upon gas-water displacement experiments. This behaviour is similar to that measured by Fishlock et al in depressurisation experiments that were performed starting with a core containing gas at waterflood residual conditions. The results suggest that gas relative permeabilities measured in gas-water displacement experiments are not directly applicable to the depressurisation of waterflooded reservoirs, and that some care may be needed in choosing gas relative permeability curves for simulating reservoir performance in these situations.

Visual observations have shown that the low values of gas relative permeability can be explained by the fact that the filaments which form the channels for gas flow are not stable, and that the flow is intermittent. As a result, the effective total area for flow is substantially reduced. In this respect, the flow characteristics when the gas is mobilised by connecting together a number of isolated bubbles may be different to those associated with gas displacement.

Network models usually assume that, once the channels have been formed they are permanently available for gas flow, and that the number of channels at any particular gas saturation is the number that was formed at a lower saturation plus the new channels formed by the increased number of pores that contain gas. The results of our experiments suggest that this assumption is not valid, and that new algorithms need to introduced into the network models to represent the cyclical nature of filament rupture and reformation, and provide suitable models for calculating gas relative permeabilities in these circumstances.

The experiments have also produced low values for the water phase relative permeabilities. Once again, this is in keeping with Fishlock et al's measurements. At this stage, however, there is no satisfactory explanation for these low values.

ACKNOWLEDGEMENTS

The authors wish to thank the Centre for Marine and Petroleum Technology for providing financial support to this project, and EPSRC for funding C.A. Grattoni.

REFERENCES

1. Kortekaas, T.F. Out Oil Reservoirs". *SPE Reservoir Engineering*, **6** (Aug. 1991), 329-335.
2. Braithwaite, C.I.M., and Schulte, W. M., "Transforming the Future of the Brent Field; Depressurisation - The Next Development Phase". Presented at the *SPE European Petroleum Conference*, Cannes, France, Nov. 1992. SPE 25026.
3. Scherpenisse, W., Wit, K., Zweers, A.E., Snoei, G., and Van Wolfswinkel, A., "Predicting Gas Saturation Build-up During Depressurisation of a North Sea Oil Reservoir". Presented to the *SPE Europec Meeting*, London, Oct. 1994. SPE 28842.
4. Ligthelm, D.J., Reijnen, G.C.A.M., Wit, K., Weisenborn, A.J., and Scherpenisse, "Gas Saturation During Depressurisation and its Importance in the Brent Field". Presented to *Offshore Europe Conference*, Aberdeen, Scotland, Sep. 1997. SPE 38475.
5. Hawes, R.I., Dawe, R.A., and Evans, R.N., "The Release of Solution Gas From Waterflooded Residual Oil". *SPE Journal*, **2** (Dec. 1997), 379-388.
6. Hawes, R.I., Dawe, R.A., Evans, R.N. and Grattoni, C.A., "The Depressurisation of Waterflooded Reservoirs: Wettability and Critical Gas Saturation". *Petroleum Geoscience*, **2** (1996), 117-123.
7. Dawe, R.A., Hawes, R.I. and Grattoni, C.A., "The Effects Of Wettability And Interfacial Forces On The Depressurisation Of Waterflooded Reservoirs", *9th European Symposium on Improved Oil Recovery*. The Hague, Netherlands, Oct.1997.
8. Hawes, R.I., Dawe, R.A., and Evans, R.N., "Theoretical Model for the Depressurisation of Water-flooded Reservoirs". *Transactions of the Institute of Chemical Eng.*, **74** (1996), part A, 197-205.

9. McDougall S.R., and Sorbie, K.S., "Estimation of Critical Gas Saturation During Pressure Depletion in Virgin and Waterflooded Reservoirs", *9th European Symposium on Improved Oil Recovery*. The Hague, Netherlands, Oct.1997.

10. Fishlock, T.P., Smith, R.A., Soper, B.M., and Wood, R.W.,"Experimental Studies on the Waterflood Residual Gas Saturation and its Production by Blowdown". *SPE Res. Eng.*, **3** (May 1988), 387-394.

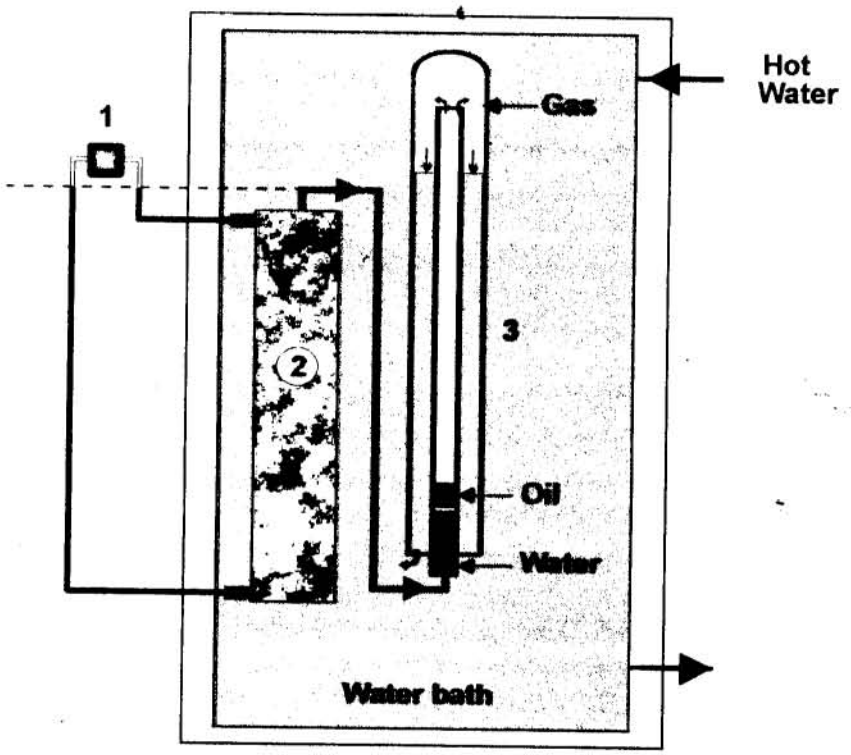

Figure 1 - Diagram of apparatus. **1**- Differential pressure transducer, **2**- Beadpack. **3**- Phase separation and measurement.

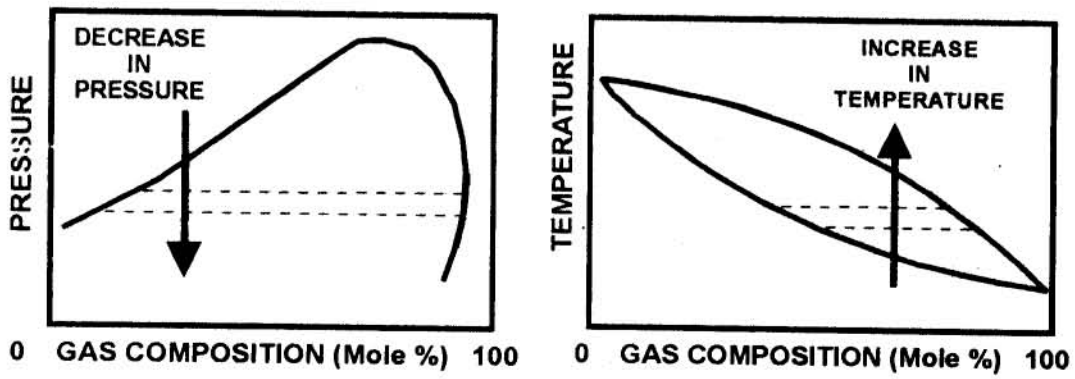

Figure 2- Techniques for solution gas release by pressure reduction and heating.
SPE Copyright, from ref. (5)

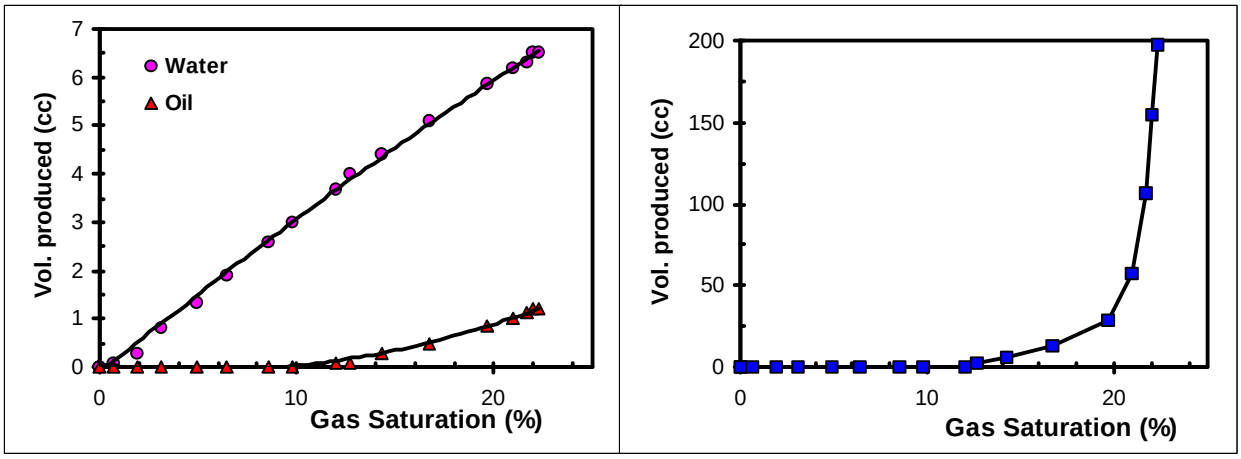

A- Water and Oil produced **B- Gas produced**

Figure 3- Cumulative effluent production data as a function of gas saturation.

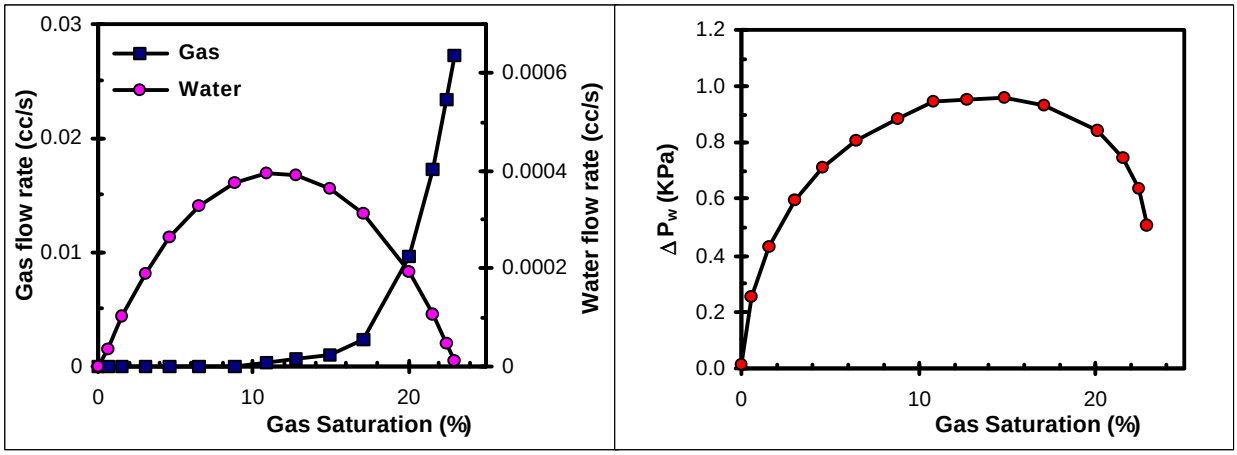

A- Water and Oil flow rates **B- Water pressure differential across the pack**

Figure 4- Production rates and differential pressure as a function of gas saturation.

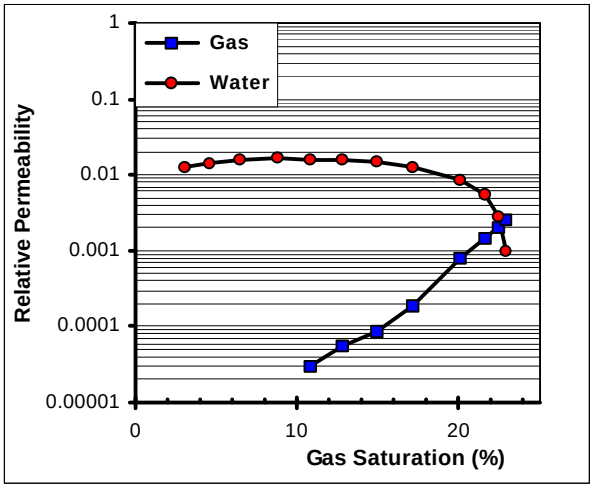

Figure 5- Experimental water and gas relative

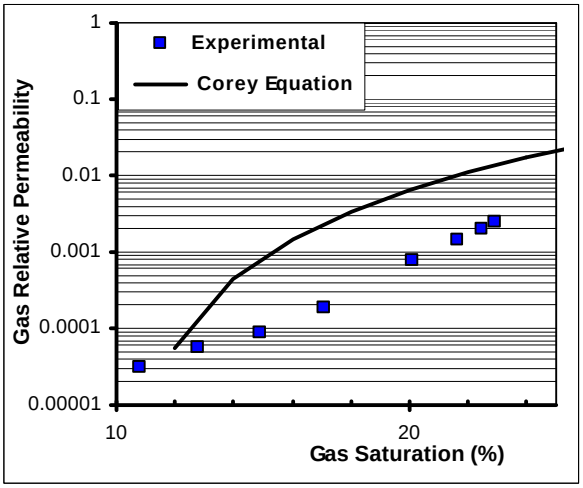

Figure 6- Comparison of gas relative

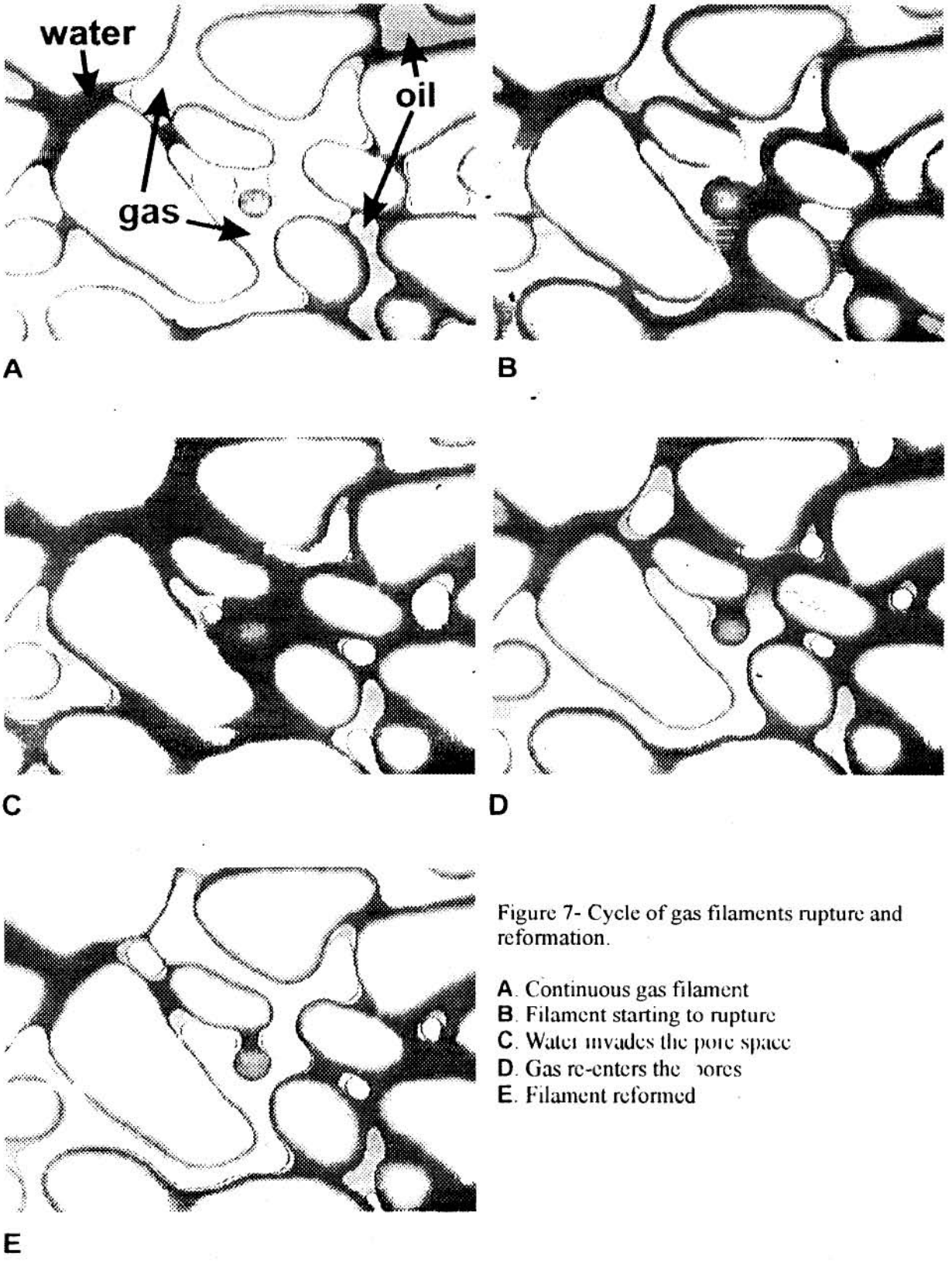

Figure 7- Cycle of gas filaments rupture and reformation.

A. Continuous gas filament
B. Filament starting to rupture
C. Water invades the pore space
D. Gas re-enters the pores
E. Filament reformed